Reduction of Cr(VI) to Cr(III) using silicon nanowire arrays under visible light irradiation

Article *in* Journal of hazardous materials · November 2015

DOI: 10.1016/j.jhazmat.2015.11.020

Dear Author,

Please, note that changes made to the HTML content will be added to the article before publication, but are not reflected in this PDF.

Note also that this file should not be used for submitting corrections.

Journal of Hazardous Materials xxx (2015) xxx–xxx

Contents lists available at ScienceDirect

Journal of Hazardous Materials

journal homepage: www.elsevier.com/locate/jhazmat

Reduction of Cr(VI) to Cr(III) using silicon nanowire arrays under visible light irradiation

Q1 Ouarda Fellahi[a,b], Alexandre Barras[a], Guo-Hui Pan[c], Yannick Coffinier[a], Toufik Hadjersi[b], Mustapha Maamache[d], Sabine Szunerits[a], Rabah Boukherroub[a,*]

[a] Institut d'Electronique, de Microélectronique et de Nanotechnologie (IEMN), UMR CNRS 8520, Avenue Poincaré—BP 70478, 59652 Villeneuve d'Ascq Cedex, France
[b] Centre de Recherche en Technologie des Semi-conducteurs pour l'Energétique-CRTSE 02, Bd Frantz Fanon, BP. 140, Alger 7 Merveilles, Algeria
[c] State Key Laboratory of Luminescence and Applications, Changchun Institute of Optics, Fine Mechanics and Physics, Chinese Academy of Sciences, 3888 Dong Nanhu Road, Changchun 130033, China
[d] Laboratoire de Physique Quantique et Systèmes Dynamiques, Département de Physique, Université de Sétif, Sétif 19000, Algeria

HIGHLIGHTS

- Cr(VI) reduction to Cr(III) using silicon nanowires decorated with Cu nanoparticles.
- The reduction takes place at room temperature and neutral pH under visible light.
- The photocatalytic reduction was enhanced by addition of adipic or citric acid.

GRAPHICAL ABSTRACT

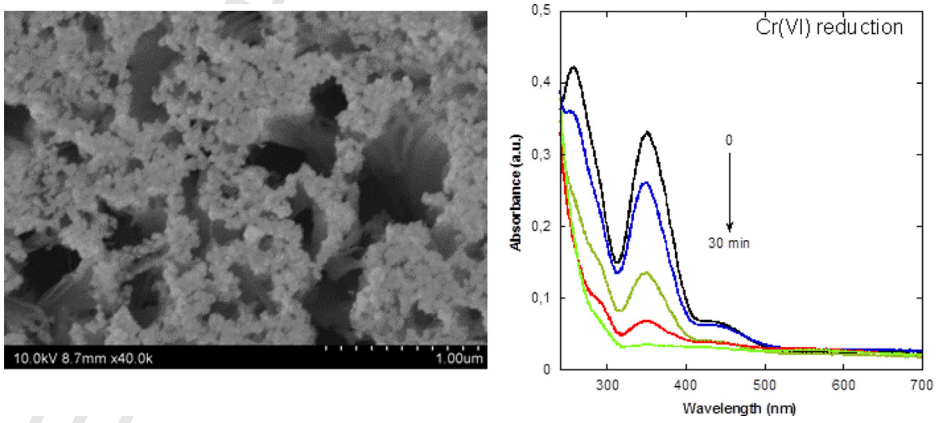

ARTICLE INFO

Article history:
Received 21 September 2015
Received in revised form
10 November 2015
Accepted 12 November 2015
Available online xxx

Keywords:
Silicon nanowires
Copper nanoparticles
Photocatalysis
Chromium(VI)
Chromium(III)
Organic acids
Visible light

ABSTRACT

We report an efficient visible light-induced reduction of hexavalent chromium Cr(VI) to trivalent Cr(III) by direct illumination of an aqueous solution of potassium dichromate ($K_2Cr_2O_7$) in the presence of hydrogenated silicon nanowires (H-SiNWs) or silicon nanowires decorated with copper nanoparticles (Cu NPs-SiNWs) substrate as photocatalyst. The SiNW arrays investigated in this study were prepared by chemical etching of crystalline silicon in $HF/AgNO_3$ aqueous solution. The Cu NPs were deposited on SiNW arrays *via* electroless deposition technique. Visible light irradiation of an aqueous solution of $K_2Cr_2O_7$ (10^{-4} M) in presence of H-SiNWs showed that these substrates were not efficient for Cr(VI) reduction. The reduction efficiency achieved was less than 10% after 120 min irradiation at $\lambda > 420$ nm. Addition of organic acids such as citric or adipic acid in the solution accelerated Cr(VI) reduction in a concentration-dependent manner. Interestingly, Cu NPs-SiNWs was found to be a very efficient interface for the reduction of Cr(VI) to Cr(III) in absence of organic acids. Almost a full reduction of Cr(VI) was achieved by direct visible light irradiation for 140 min using this photocatalyst.

Q2 * Corresponding author. Fax: +33 3 62 53 17 01.
E-mail addresses: rabah.boukherroub@iemn.univ-lille1.fr, rabah.boukherroub@univ-lille1.fr (R. Boukherroub).

http://dx.doi.org/10.1016/j.jhazmat.2015.11.020
0304-3894/

1. Introduction

Hexavalent chromium Cr(VI) is a priority pollutant in many countries and Cr(VI) contamination of soil and groundwater is a significant problem worldwide [1]. The extensive distribution of this pollutant in the environment is due primarily to its application in a wide range of industries such as the production of stainless steel, in plating, refractory industry and tanning of leather, pigment and chemical industry, wood treatment, *etc.* Cr(VI) is toxic to humans, animals, plants and microorganisms. In contrast, Cr(III) is much less toxic and an essential nutrient for human and animals; Cr(VI) reduction to Cr(III) is thus very important in the remediation of environmental sites contaminated by chromium. Several research reports have focused on the reduction of Cr(VI) to Cr(III) using semiconductor catalysts such as TiO_2 [2–4], WO_3-doped TiO_2 nanotubes [4], $NaTaO_3$ [5], NiO/TiO_2 [5], ZnO/TiO_2 composite [6], NiO [7] and bismuth oxychloride [8] or ZnO nanoparticles [9] under UV or laser irradiation. The photocatalytic reduction of Cr(VI) can also be achieved under visible light irradiation when nanocomposites of TiO_2 and SnS_2 [10], bismuth-doped ordered mesoporous TiO_2 [11], TiO_2/graphene [12], SnS_2/SnO_2 [13] nanocomposite, N-doped TiO_2 [14], and g-C_3N_4 [15] are used as photocatalysts.

When a semiconductor suspension was irradiated with UV light ($\lambda < 387$ nm), the photo-induced electrons are responsible for the photocatalytic reduction of Cr(VI). The UV or visible photocatalytic reduction of Cr(VI) to Cr(III) generally proceeds very slowly, because the accompanying oxidation of water to oxygen is a kinetically slow process [16]. Addition of organic donors accelerates significantly the UV photocatalytic reduction of Cr(VI), due to enhanced charge separation of photo-induced hole/electron pairs by the simultaneous reduction/oxidation reactions [17–21].

Although bulk silicon displays a small band gap (~1.1 eV), it has so far not been investigated in heterogeneous photocatalysis because its valence band is not positive enough to oxidize organic pollutants. In the last years, it has been established that silicon in its nanostructured form is, however, an effective photocatalyst for oxidation of organic dyes and selective oxidation of aromatic molecules [22–29], as well as for the reduction of graphene oxide (GO) [30]. The photocatalytic efficiency of hydrogenated SiNWs for the degradation of rhodamine B (RhB) and oxidation of benzyl alcohol to benzoic acid was highlighted for the first time by Shao et al. [23]. The higher performance of H-SiNWs compared to SiNWs decorated with Pd, Au, Rh or Ag NPs for the degradation of RhB was also demonstrated [23]. We have recently shown that decorating SiNWs with Cu NPs enhances the photocatalytic performance of the substrate for the photodegradation of RhB under visible light irradiation [24].

While the photocatalytic activity of SiNWs substrates for the oxidation of dyes and organic molecules has been described, there has been no report on the use of these substrates for the reduction of hexavalent chromium Cr(VI) under visible light irradiation. The goal of our work is to investigate the efficiency of SiNWs catalysts for the photoreduction of Cr(VI) to Cr(III) under visible light irradiation with and without organic additives. The photocatalysts consist of H-SiNWs and SiNWs decorated with Cu NPs. In the absence of organic additives, it was found that H-SiNWs was not efficient for the Cr(VI) reduction under visible light irradiation, while Cu NPs-SiNWs led to almost full reduction of Cr(VI) after 140 min irradiation. Addition of citric acid (5 mM) into the solution accelerated significantly the reduction rate.

2. Results and discussion

The SiNW arrays investigated in this study are obtained by metal-assisted chemical etching of p-type silicon wafers (boron-doped, 0.009–0.01 Ω-cm resistivity) in HF (5 M)/$AgNO_3$ (0.035 M) aqueous solution at 55 °C for 30 min [30–32]. The technique is easy to carry out and the formation of the silicon nanostructures takes place at relatively low temperature. As shown in scanning electron microscopy (SEM) images in Fig. 1, this one step chemical etching process produces vertically oriented SiNWs with a length of ~5.6 μm and a diameter size in the range of 20–100 nm (Fig. 1A and B). EDX analysis of H-SiNWs substrate shows a strong signal from Si element and a small contribution from oxygen (Fig. 1C). The presence of oxygen in the EDX spectrum is most likely due to partial oxidation of silicon upon exposure to ambient.

Cu-decorated SiNW arrays are prepared by the electroless deposition technique [24,30,33]. In aqueous solutions, metal ions with redox potential greater than hydrogen attract electrons from Si atoms and are reduced to the atomic form. In diluted HF-solutions, Cu adheres on the Si surface easily and deposits locally in a particle form [34]. This technique has been applied for deposition of Cu nanostructures on porous silicon [35,36]. Electroless deposition of Cu on SiNW arrays occurs according to the following cathodic reaction:

$$Cu^{2+} + 2e^- \rightarrow Cu(s)$$

The deposited metal atoms first form nuclei and then nanoclusters to give nanoparticles. This reaction is accompanied by silicon oxidation:

$$Si + 2H_2O \rightarrow SiO_2 + 4H^+ + 4e^-$$

The role of HF in this chemical process is to dissolve the SiO_2 layer. Fig. 1D and E displays SEM images of the resulting SiNWs substrates decorated with Cu nanoparticles. Because of the concentration gradient of metal ions, more nanoparticles tend to grow at the tips of the nanowires [37]. Thus, the metal nanoparticles aggregate and grow larger, while the SiNWs become tapered. From the top-view SEM image in Fig. 1D, one sees that the nanowires are stuck to each other to form bundles. This phenomenon is most likely due to van der Waals attraction between the nanowires upon drying. Alternatively, it was also suggested that some nanowires may be left undetached due to inhomogeneous etching induced by a random Ag particle distribution [38]. A high magnification SEM image suggests that the size of the surface-deposited Cu NPs is in the range of ~50–100 nm (Fig. 1E). In contrast to H-SiNWs, the EDX spectrum of the Cu NPs-SiNWs substrate exhibits signals due to Si and Cu, and a small contribution from oxygen (Fig. 1F). The results are in good agreement with copper deposition on the nanowires. The presence of oxygen in the EDX spectrum is most likely due to partial oxidation of silicon upon exposure to ambient.

For TEM imaging analysis, the as-etched SiNWs or Cu NPs-SiNWs were scratched from the silicon substrate carefully and then were dispersed in ethanol by ultrasonication. Fig. S1 displays the TEM images of SiNWs. One SiNW of up to ~2.5 μm in length and ~150 nm in diameter was imaged in Fig. S1A. However, a closer observation on a selective area of this long SiNW (inset of Fig. S1A) indicates that the nanowire is porous with pore diameter of ~10 nm. In addition, some much shorter SiNWs or agglomerated/porous particles always appear upon extensive TEM observation, which most probably due to the breaking of as-etched SiNW during post-treatment consisting of scratching and ultrasonication. The high resolution TEM image taken on the long SiNW clearly shows the lattice fringes of diamond-like silicon (Fig. S1B). The interplanar spacing of ~0.31 nm is in good agreement with the *d*-spacing of (1 1 1) crystalline plane. SAED analysis is also performed on the SiNW. In most cases, the patterns consist of many regularly arranged diffraction spots, which imply the single crystallinity of the SiNWs even though they are porous. Such a feature

Please cite this article in press as: O. Fellahi, et al., Reduction of Cr(VI) to Cr(III) using silicon nanowire arrays under visible light irradiation, J. Hazard. Mater. (2015), http://dx.doi.org/10.1016/j.jhazmat.2015.11.020

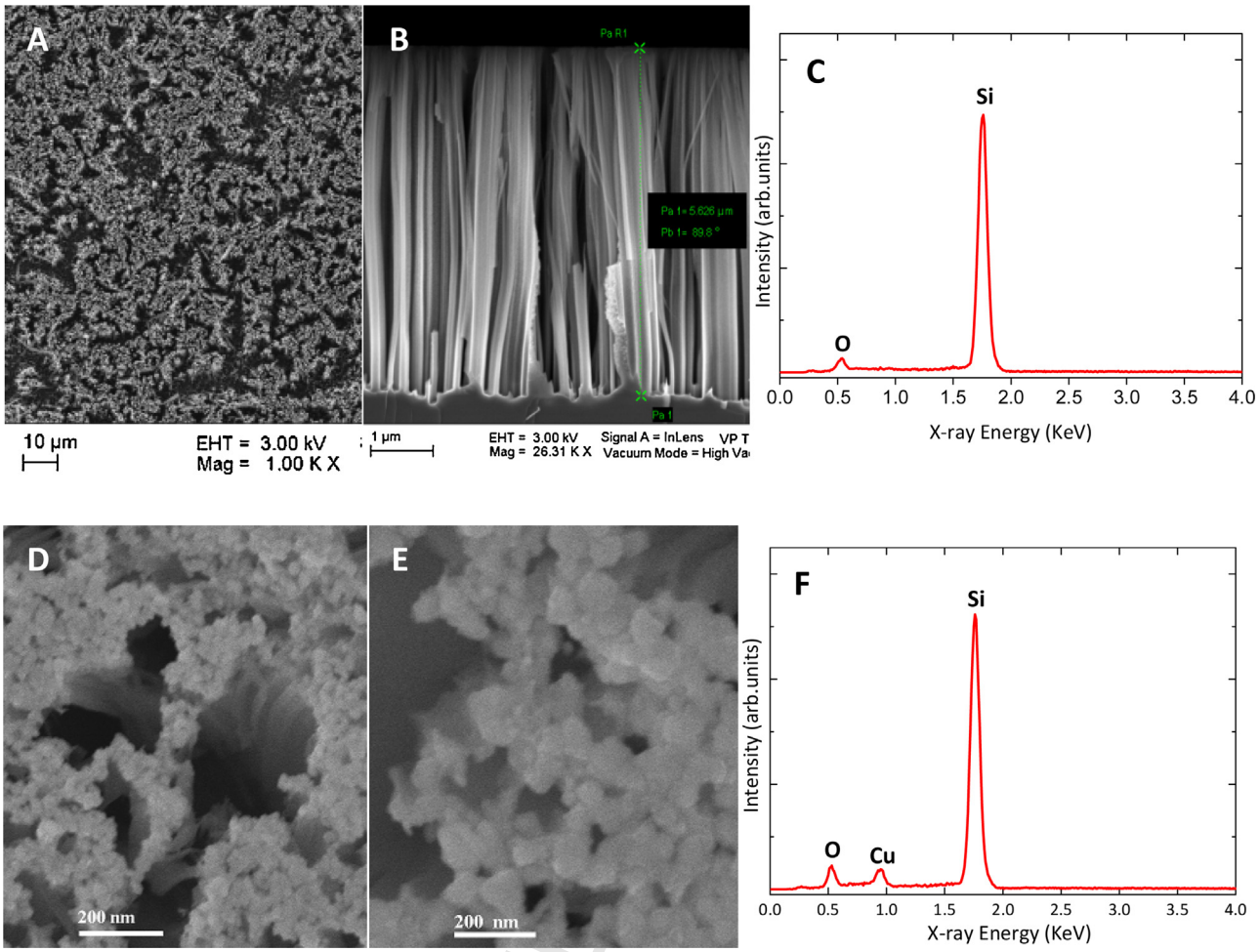

Fig. 1. Top view (A) and cross-sectional (B) SEM images of silicon substrate etched in an aqueous solution of HF (5 M)/$AgNO_3$ (0.035 M) for 30 min at 55 °C; (C) energy dispersive X-ray spectra of H-SiNWs; (D) top view SEM image of Cu NPs-SiNWs; Cu NPs deposition was achieved using $CuCl_2$ (0.035 M)/HF (1.45 M) aqueous solutions for 1 min at room temperature; (E) high magnification SEM image of the surface deposited Cu NPs; (F) energy dispersive X-ray spectra of Cu NPs-SiNWs.

is actually reasonable since the SiNWs were prepared by chemical etching of bulk silicon single-crystal wafer. A representative SAED pattern is shown in Fig. S1C. The index to some diffraction spots were indicated therein.

Fig. 2 exhibits the TEM images of Cu NPs-SiNWs. A bundle of SiNWs appears in Fig. 2A. This agrees well with the SEM observations of as-etched SiNWs on the silicon substrate. In addition, some separated particles and SiNWs are also observed. However, most of these agglomerated particles are silicon upon careful analysis by high-resolution TEM combined with fast Fourier transformation (FFT). Cu NPs are less observed due to their small amounts relative to SiNWs. Moreover, single/separated Cu NPs are yet less observed, in most cases present as aggregates with silicon particles, but with much higher contrast (darker than surrounding silicon) due to the higher atomic number (Z) contrast relative to the underlying carbon support. Fig. 2B shows one ~50 nm Cu NP in the black frame aggregated with silicon particles. High resolution TEM image on its edge reveals the lattice fringes of crystalline cubic copper (Fig. 2C). The d-spacing of 0.22 nm corresponds to the interplanar distance of (1 1 1) plane. The SAED pattern recorded on this Cu NP consists of homocentric rings, indicating the polycrystallinity (Fig. 2D). From the inner to outer, the rings could be indexed to (1 0 0), (1 1 1) and (2 0 0) crystalline planes.

The photoreduction of Cr(VI) using H-SiNWs substrates was conducted under visible light irradiation ($\lambda > 420$ nm; power = 0.9 W cm^{-2}) at room temperature by immersion of the H-SiNW substrate into a 2 mL aqueous solution of potassium dichromate ($K_2Cr_2O_7$) with an initial concentration of 10^{-4} M. An aqueous solution of Cr(VI) displays two main absorption features at around 257 and 352 nm (Fig. 3A). The photocatalytic reduction process was monitored by the decay of the absorption band at 352 nm as a function of irradiation time. Direct irradiation (*i.e.*, without SiNWs) of a 10^{-4} M aqueous solution of Cr(VI) under visible light irradiation for 120 min did not show any apparent change in the UV/vis spectrum, suggesting that Cr(VI) is very stable under these photocatalytic conditions. Visible light irradiation of the Cr(VI) solution in the presence of H-SiNWs led to a decrease of the absorption band intensity of less than 10% after 120 min under otherwise identical experimental conditions. This slight decrease of the absorption is most likely due to Cr(VI) ions adsorption on the substrate rather than from its catalytic reduction stimulated by visible light. The results suggest that H-SiNWs substrate is not an efficient photocatalyst for Cr(VI) reduction under visible light irradiation.

Interestingly, when the reduction of Cr(VI) is performed in the presence of Cu NPs-SiNWs substrate, an almost full reduction of Cr(VI) after 140 min irradiation is observed (Fig. 3A). The reduction of Cr(VI) is a complex process as can be seen from Fig. 3A. It is to be noted that the decrease of the absorption by ~10% in the first 20 min is due to Cr(VI) adsorption on the SiNWs surface since the solution was not irradiated. We have noticed that 20 min were sufficient to reach the equilibrium and no further decrease is observed

Please cite this article in press as: O. Fellahi, et al., Reduction of Cr(VI) to Cr(III) using silicon nanowire arrays under visible light irradiation, J. Hazard. Mater. (2015), http://dx.doi.org/10.1016/j.jhazmat.2015.11.020

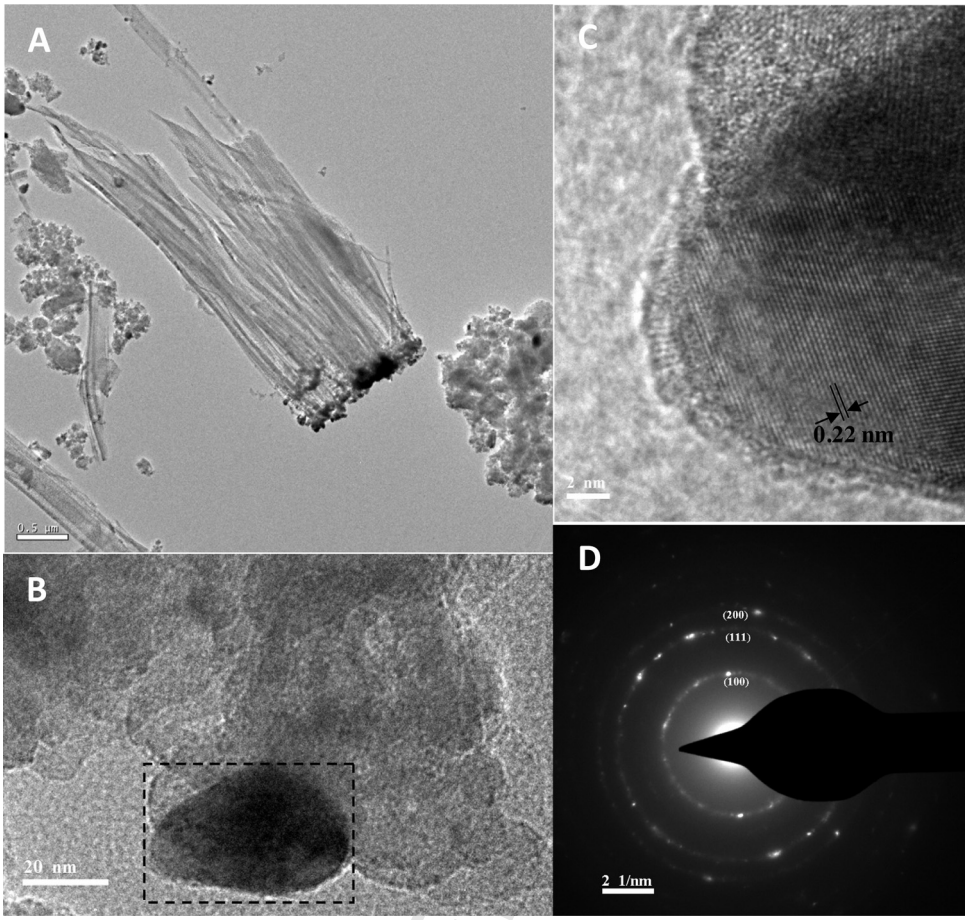

Fig. 2. (A) TEM image of Cu NPs-SiNWs scratched from the silicon substrate; (B) high magnification TEM image of aggregated silicon NPs and one Cu NP in the black frame; (C) high-resolution TEM image taken near the edge of Cu NP present in Fig. 3B; (C) SAED pattern recorded from the Cu NP present in Fig. 3B.

for longer exposure times without irradiation. Visible light irradiation for 20 min led to the shift of the absorbance peaks of Cr(VI) from 257 to 271 nm and from 352 to 370 nm, respectively, without any evident decrease of their intensity (Fig. 3A). No further red shift is observed after 20 min irradiation. However, the absorbance decreased in a quick manner to reach a value <5% for the two peaks after 140 min irradiation (Fig. 3B).

We have next studied the effect of organic acid (adipic or citric acid) additives on the Cr(VI) reduction upon visible light irradiation in the presence of H-SiNWs. Addition of adipic acid (5 mM) into an aqueous solution of Cr(VI) (10^{-4} M) in the presence of H-SiNWs accelerated significantly the reduction rate (Fig. 4A). Indeed, after 240 min visible light irradiation about 55% of Cr(VI) is reduced. Decreasing adipic acid concentration to 0.5 and 0.05 mM resulted in a decrease of the performance of the photocatalyst with 26 and 34% of Cr(VI) reduction, respectively after 240 min irradiation. In control experiments, we have checked the effect of adipic acid on Cr(VI) upon storage in the dark and visible light irradiation. While dark storage of 10^{-4} Cr(VI) aqueous solutions containing adipic acid (0.05, 0.5 or 5 mM) at room temperature for 20 h did not show obvious changes in the Cr(VI) content (Fig. S2A), visible light irradiation of the same solutions for 240 min induced about 7% reduction of Cr(VI) (Fig. S3).

Similarly, we have undertaken the photoreduction reaction of Cr(VI) in the presence of citric acid at 0.05, 0.5 and 5 mM using H-SiNWs as photocatalyst (Fig. 4B). Compared to adipic acid, the reduction process was much more enhanced with a complete reduction of Cr(VI) after 240 min irradiation when 5 mM of citric acid was used. For citric acid concentrations of 0.5 and 0.05 mM, 80 and 22% of Cr(VI) were reduced, respectively upon 240 min visible light irradiation. Controls consisting of dark or visible light irradiation of Cr(VI) in the presence of citric acid suggested that no reduction occurred upon dark storage for 20 h at room temperature (Fig. S2B), while visible light irradiation caused ~27% reduction in the presence of 5 mM citric acid (Fig. S3).

Furthermore, we have investigated the effect of 5 mM citric acid on the photocatalytic reduction of Cr(VI) in the presence of Cu NPs-SiNWs substrate under visible light irradiation. UV–vis absorption results indicated that almost a full reduction of Cr(VI) was achieved only after 30 min irradiation (Fig. 5). Addition of citric acid accelerated significantly the reduction when Cu NPs-SiNWs substrate was used as photocatalyst.

From these results, we can notice that the influence of adipic acid on the reduction rate of Cr(VI) is somehow different from that of citric acid. Although, the result is not very clear at this stage, it has been postulated in the literature that organics capable of donating electrons directly to the valence band of the photocatalyst result in high reduction rates, while those that are oxidized only by hydroxyl radicals produce lower rates [39]. In the former case, electrons from the organics rapidly fill valence band holes, limiting electron/hole recombination leaving more conduction-band electrons available for Cr(VI) reduction. In the latter, holes are only filled by the formation of hydroxyl radicals; thus, organics affect reduction indirectly, resulting in slow reduction.

The reproducibility of the Cu NPs-SiNWs for the photocatalytic reduction of Cr(VI) was investigated using 3 different samples prepared under the same experimental conditions. The photocatalytic reduction of Cr(VI) in the presence of 5 mM citric acid and Cu

Please cite this article in press as: O. Fellahi, et al., Reduction of Cr(VI) to Cr(III) using silicon nanowire arrays under visible light irradiation, J. Hazard. Mater. (2015), http://dx.doi.org/10.1016/j.jhazmat.2015.11.020

NPs-SiNWs substrate under visible light irradiation gave almost full reduction of Cr(VI) to Cr(III) after 30 min irradiation, indicating a good reproducibility of the fabrication method. The stability of the Cu NPs-SiNWs was assessed through three consecutive photocatalytic runs for the reduction of a 10^{-4} M aqueous solution of Cr(VI) in the presence of 5 mM citric acid. While almost a full reduction of Cr(VI) to Cr(III) was observed after 30 min for the two first cycles, the third cycle required much longer time (115 min) to achieve full reduction. The slight deactivation of the photocatalyst is most likely due to Cr(III) adsorption on the photocatalyst surface [20].

One practical limitation in photocatalytic reactions using semiconductors is the undesired fast electron/hole recombination, which, in the absence of electron donor or acceptor is extremely efficient. It has previously been proposed that the Si—H bonds present on the H-SiNWs surface can serve as electron traps and can accelerate the separation between (electron–hole) and consequently increases the photocatalytic activity of the photocatalyst [23]. Furthermore, the deposition of metal particles (Au, Ag, Pt, Pd or Cu) on the surface of SiNW substrates increases the catalytic activity for the photodegradation of organic pollutants [23,24]. These heterostructures cause the trapping of electrons photo-generated in the metal, reducing the possibility of electron–hole recombination.

A plausible mechanism for the photocatalytic reduction of Cr(VI) over SiNWs photocatalysts under visible light can be summarized as follows:

$$\mathrm{SiNWs} + h\nu \rightarrow \mathrm{SiNWs}(h^+ + e^-) \quad (1)$$

$$Cr_2O_7^{2-} + 14H^+ + 6e^- \rightarrow 2Cr^{3+} + 7H_2O \quad (2)$$

$$H_2O + h^+ \rightarrow OH^\bullet + H^+ \quad (3)$$

$$Cr^{3+} + 2h^+ + OH^\bullet \rightarrow Cr^{6+} + OH^- \quad (4)$$

An electron–hole pair is generated upon excitation of the SiNWs substrate with a photon of energy equal to or higher than the band gap (E_g ~1.1 eV) (Eq. (1)). Reaction of the photoexcited catalyst with H_2O (*i.e.*, oxidative hole trapping) creates "surface" bound •OH radicals (Eq. (3)). Subsequent reaction of Cr(III) with holes or

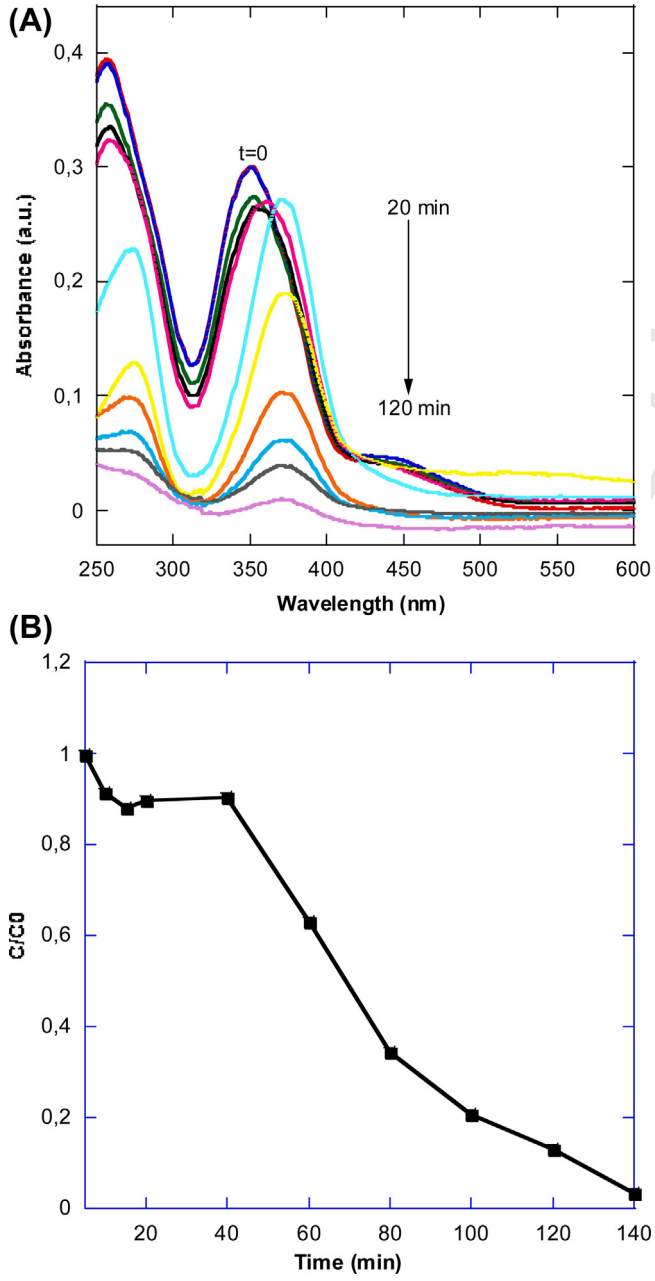

Fig. 3. (A) UV/vis spectra and (B) temporal course of the photocatalytic reduction of 10^{-4} M $K_2Cr_2O_7$ aqueous solution in the presence Cu NPs-SiNWs.

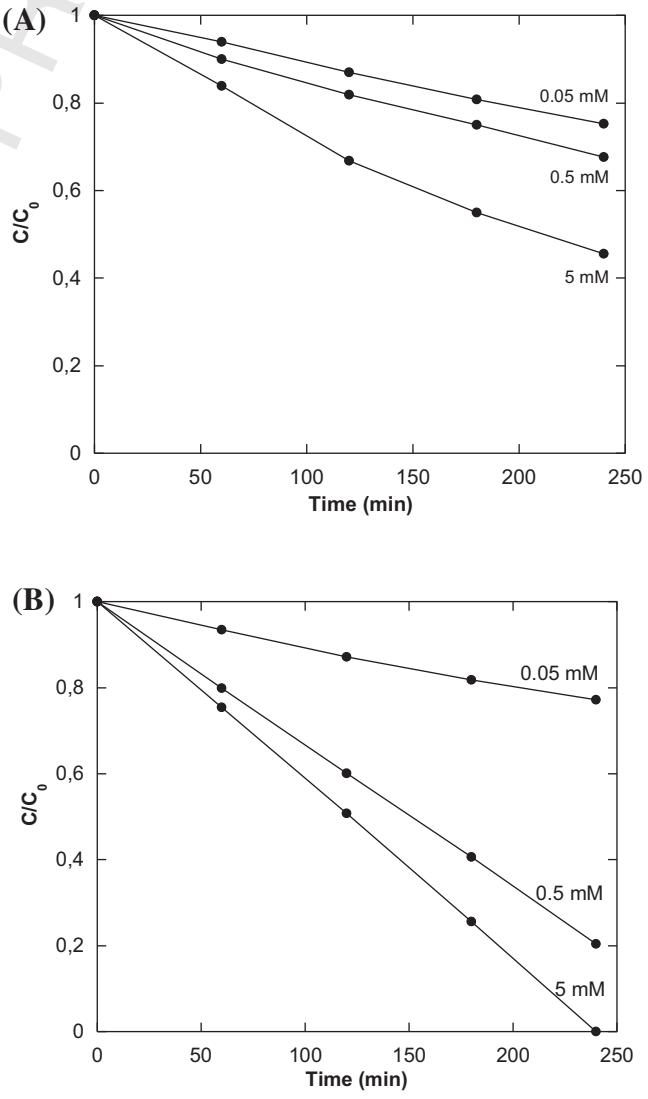

Fig. 4. Temporal course of the photocatalytic reduction of 10^{-4} M $K_2Cr_2O_7$ aqueous solution in the presence of H-SiNWs and different concentrations of adipic acid (A) and citric acid (B).

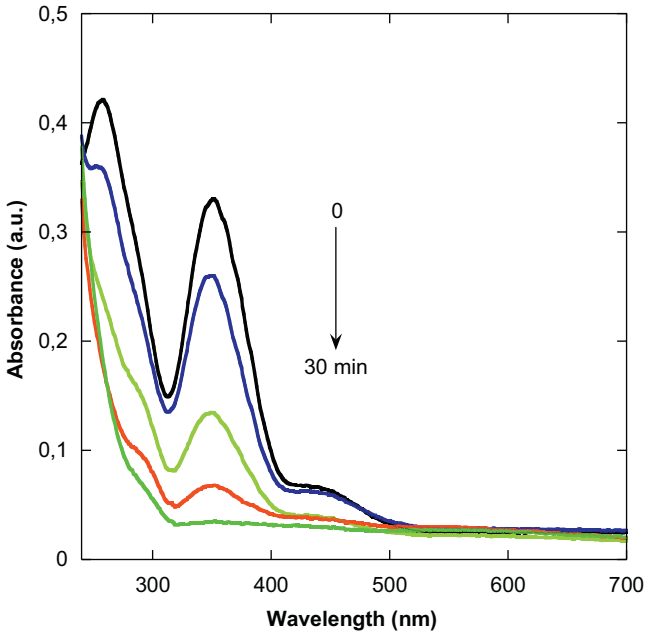

Fig. 5. UV–vis absorption spectra of the photocatalytic reduction of 10^{-4} M $K_2Cr_2O_7$ aqueous solution in the presence of 5 mM citric acid and Cu NPs-SiNWs.

hydroxyl radicals leads to its reoxidation back to Cr(VI) (Eq. (4)). In the absence of organic acids, we found that the photocatalytic activity of H-SiNWs is low for the reduction of Cr(VI) contained in the solution of potassium dichromate. This is probably due to fast electron/hole recombination or ascribed to a short-circuiting due to the continuous reduction and reoxidation of chromium species by holes or hydroxyl radicals (Eq. (4)) [3,4,17]. However, upon decoration with copper nanoparticles, an increase in the number of trapped electrons enhances the catalytic performance of the catalyst. The electrons can be scavenged by Cr(VI), which in turn is reduced to Cr(III) (Eq. (2)). In addition, because Cu can be easily oxidized in open air, Cu oxide phase can be formed on Cu nanoparticles and promotes the production of hydroxyl radicals •OH (Eq. (3)), that are strong oxidizing agents for organic pollutants [40,41]. This process consumes the holes thereby preventing the electron–hole recombination on SiNWs.

The chemical composition of the as-prepared Cu NPs-SiNWs substrate and after photocatalytic use was examined using X-ray photoelectron spectroscopy (XPS). The high resolution of the core level of Cu 2p of the as-prepared Cu NPs-SiNWs substrate reveals the presence two main peaks at 932.68 and 952.48 eV due to Cu $2p_{3/2}$ and Cu $2p_{1/2}$, respectively from metallic Cu^0 or Cu^+ (Cu_2O) (Fig. S4A). Unfortunately, Cu^0 cannot be distinguished from Cu^+ by XPS because of their spectral overlap [42,43]. However, based on the literature data, the peak is most likely due to Cu^0 (the ISO standard Cu metal line is at 932.63 eV with a deviation set at ±0.025 eV) [43,44]. The overall Cu content is 24.8 at%, indicating high loading of Cu NPs onto the SiNWs surface. Fig. S4B displays the core level of Cu 2p of the Cu NPs-SiNWs substrate after photocatalytic use. It comprises two main peaks at 934.1, 953.89 eV and two satellite peaks at 944.55 and 964.22 eV. The peaks at 934.1 and 953.89 eV are due to Cu $2p_{3/2}$ and Cu $2p_{1/2}$, respectively from Cu^{2+}. In addition, the presence of shake-up satellite peaks at higher binding energies *i.e.*, 944.55 and 964.22 eV, characteristic of materials having a d^9 configuration in their ground state, clearly indicates the presence of Cu^{2+} [43]. The results clearly indicate the presence of Cu oxide phase on the photocatalyst.

Addition of organic acids promoted and enhanced significantly Cr(VI) reduction in the presence SiNWs-based photocatalysts. Indeed, in the presence of degradable organic pollutants, the holes can produce •OH radicals (Eq. (3)), which can further degrade the organics to CO_2 and H_2O (Eq. (5)). Of course, the holes can also directly oxidize the organic molecules (Eq. (6)). In other words, in the presence of organic acids, the photogenerated holes are rapidly scavenged from the SiNWs, suppressing electron–hole recombination on SiNWs and accelerating the reduction of Cr(VI) by photogenerated electrons [45]. Such a synergistic effect between the photocatalytic reduction of Cr(VI) and the oxidation of organic compounds was also reported by Wang et al. using TiO_2 as photocatalyst [19].

$$\text{•OH} + \text{organics} \rightarrow \cdots \rightarrow CO_2 + H_2O \quad (5)$$

$$h^+ + \text{organics} \rightarrow \cdots \rightarrow CO_2 + H_2O \quad (6)$$

Moreover, we have performed several controls to gain further insights into the red shift of the Cr(VI) absorption peaks upon visible light irradiation in the presence of Cu NPs-SiNWs photocatalyst. This red shift did not occur on both hydrogenated SiNWs and oxidized SiNWs upon 120 min visible light irradiation, although no Cr(VI) reduction was achieved using these photocatalysts. This means that the Cu NPs are involved in the red shift of Cr(VI) absorption peaks. To this end, equimolar solutions of Cr(VI) and Cu(II) were irradiated under visible light for 20 min. No red shift or absorption decrease was observed under these experimental conditions. Similar results were obtained upon 20 min visible light irradiation of an aqueous solution of 10^{-4} M Cr(VI) saturated with CuBr. The results suggest that these species, even present in the solution, are not responsible for the red shift observed upon visible light irradiation of Cr(VI). Upon exposure to air (and in aqueous solution), Cu can be easily oxidized to Cu oxide. Thus, the formation of Cr(VI) complex with —OH groups on the surface cannot be excluded. However at this stage, it is difficult to draw a final conclusion on the red shift observed in the UV–vis of Cr(VI) over Cu NPs-SiNWs. Further experiments are needed to elucidate this process.

3. Conclusion

We have demonstrated that SiNW arrays can be successfully used as high performant photocatalyst for Cr(VI) reduction under visible light irradiation. While a hydrogenated SiNWs substrate alone was not efficient in this photocatalytic process, addition of organic acids promoted Cr(VI) reduction under visible light irradiation. SiNWs decorated with copper nanoparticles, on the other hand, allows Cr(VI) reduction to Cr(III) without additives under visible irradiation. The photocatalyst can be reused two times without any obvious change in its photocatalytic activity. However, in absence of organic acids, a red shift of the absorption peaks of Cr(VI) was observed using Cu NPs-SiNWs. This shift cannot be explained at this stage and further experiments are required to elucidate this process. The preparation of SiNWs by chemical etching is simple, straightforward, cost-effective and easily scalable. The results provided in this work are very promising in view of various photocatalytic applications of the SiNWs-based substrates.

Acknowledgments

The authors acknowledge gratefully the Centre National de la Recherche Scientifique (CNRS), the Université Lille1 and the Nord Pas de Calais region for financial support.

Appendix A. Supplementary data

Supplementary data associated with this article can be found, in the online version, at http://dx.doi.org/10.1016/j.jhazmat.2015.11.020.

References

[1] X.-R. Xu, H.-B. Li, X.-Y. Li, J.-D. Gu, Reduction of hexavalent chromium by ascorbic acid in aqueous solutions, Chemosphere 57 (2004) 609–613.
[2] N. Wang, L. Zhu, K. Deng, Y. She, Y. Yu, H. Tang, Visible light photocatalytic reduction of Cr(VI) on TiO_2 in situ modified with small molecular weight organic acids, Appl. Catal. B: Environ. 95 (2010) 400–407.
[3] J.M. Meichtry, M. Brusa, G. Mailhot, M.A. Grela, M.I. Litter, Heterogeneous photocatalysis of Cr(VI) in the presence of citric acid over TiO_2 particles: relevance of Cr(V)–citrate complexes, Appl. Catal. B: Environ. 71 (2007) 101–107.
[4] L. Yang, Y. Xiao, S. Liu, Y. Li, Q. Cai, S. Luo, G. Zeng, Photocatalytic reduction of Cr(VI) on WO_3 doped long TiO_2 nanotube arrays in the presence of citric acid, Appl. Catal. B: Environ. 94 (2010) 142–149.
[5] Y. Ku, C.-N. Lin, W.-M. Hou, Characterization of coupled NiO/TiO_2 photocatalyst for the photocatalytic reduction of Cr(VI) in aqueous solution, J. Mol. Catal. A 349 (2011) 20–27.
[6] M. Naimi-Joubani, M. Shirzad-Siboni, J.-K. Yang, M. Gholami, M. Farzadki, Photocatalytic reduction of hexavalent chromium with illuminated ZnO/TiO_2 composite, J. Ind. Eng. Chem. 22 (2015) 317–323.
[7] M. Qamar, M.A. Gondal, Z.H. Yamani, Synthesis of nanostructured NiO and its application in laser-induced photocatalytic reduction of Cr(VI) from water, J. Mol. Catal. A 341 (2011) 83–88.
[8] M. Qamar, Z.H. Yamani, Bismuth oxychloride-mediated and laser-induced efficient reduction of Cr(VI) in aqueous suspensions, Appl. Catal. A 439–440 (2012) 187–191.
[9] M. Qamar, M.A. Gondal, Z.H. Yamani, Laser-induced efficient reduction of Cr(VI) catalyzed by ZnO nanoparticles, J. Hazard. Mater. 187 (2011) 258–263.
[10] Y.C. Zhang, J. Li, H.Y. Xu, One-step in situ solvothermal synthesis of SnS_2/TiO_2 nanocomposites with high performance in visible light-driven photocatalytic reduction of aqueous Cr(VI), Appl. Catal. B: Environ. 123–124 (2012) 18–26.
[11] S. Sajjad, S.A.K. Leghari, F. Chen, J. Zhang, Bismuth-doped ordered mesoporous TiO_2: visible-light catalyst for simultaneous degradation of phenol and chromium, Chem. Eur. J. 16 (2010) 13795–13804.
[12] K. Zhang, K.C. Kemp, V. Chandra, Homogeneous anchoring of TiO_2 nanoparticles on graphene sheets for waste water treatment, Mater. Lett. 81 (2012) 127–130.
[13] Y.C. Zhang, L. Yao, G. Zhang, D.D. Dionysiou, J. Li, X. Du, One-step hydrothermal synthesis of high-performance visible-light-driven SnS_2/SnO_2 nanoheterojunction photocatalyst for the reduction of aqueous Cr(VI), Appl. Catal. B 144 (2014) 730–738.
[14] Y.C. Zhang, M. Yang, G. Zhang, D.D. Dionysiou, HNO_3-involved one-step low temperature solvothermal synthesis of N-doped TiO_2 nanocrystals for efficient photocatalytic reductionof Cr(VI) in water, Appl. Catal. B 142–143 (2013) 249–258.
[15] Y.C. Zhang, Q. Zhang, Q. Shi, Z. Cai, Z. Yang, Acid-treated g-C_3N_4 with improved photocatalytic performance in the reduction of aqueous Cr(VI) under visible-light, Sep. Purif. Technol. 142 (2015) 251–257.
[16] J.J. Testa, M.A. Grela, M.I. Litter, Heterogeneous photocatalytic reduction of chromium(VI) over TiO_2 particles in the presence of oxalate: involvement of Cr(V) species, Environ. Sci. Technol. 38 (2004) 1589–1594.
[17] J.J. Testa, M.A. Grela, M.I. Litter, Experimental evidence in favor of an initial one-electron-transfer process in the heterogeneous photocatalytic reduction of chromium(VI) over TiO_2, Langmuir 17 (2001) 3515–3517.
[18] J.-K. Yang, S.-M. Lee, Removal of Cr(VI) and humic acid by using TiO_2 photocatalysis, Chemosphere 63 (2006) 1677–1684.
[19] L. Wang, N. Wang, L. Zhu, H. Yu, H. Tang, Photocatalytic reduction of Cr(VI) over different TiO_2 photocatalysts and the effects of dissolved organic species, J. Hazard. Mater. 152 (2008) 93–99.
[20] N. Wang, Y. Xu, L. Zhu, X. Shen, H. Tang, Reconsideration to the deactivation of TiO_2 catalyst during simultaneous photocatalytic reduction of Cr(VI) and oxidation of salicylic acid, J. Photochem. Photobiol. A 201 (2009) 121–127.
[21] N. Wang, L. Zhu, Y. Huang, Y. She, Y. Yu, H. Tang, Drastically enhanced visible-light photocatalytic degradation of colorless aromatic pollutants over TiO_2 via a charge–transfer-complex path: a correlation between chemical structure and degradation rate of the pollutants, J. Catal. 266 (2009) 199–206.
[22] Z. Kang, C.H.A. Tsang, N.-B. Wong, Z. Zhang, S.-T. Lee, Silicon quantum dots: a general photocatalyst for reduction, decomposition, and selective oxidation reactions, J. Am. Chem. Soc. 129 (2007) 12090–12091.
[23] M. Shao, L. Cheng, X. Zhang, D. Duo Duo Ma, S.-T. Lee, Excellent photocatalysis of HF-treated silicon nanowires, J. Am. Chem. Soc. 131 (2009) 17738–17739.
[24] N. Megouda, Y. Cofininier, S. Szunerits, T. Hadjersi, O. ElKechai, R. Boukherroub, Photocatalytic activity of silicon nanowires under UV and visible light irradiation, Chem. Commun. 47 (2011) 991–993.
[25] Y. Liu, G. Ji, J. Wang, X. Liang, Z. Zuo, Y. Shi, Fabrication and photocatalytic properties of silicon nanowires by metal-assisted chemical etching: effect of H_2O_2 concentration, Nanoscale Res. Lett. 7 (2012) 663.
[26] W. Gao, M. Shao, L. Yang, S. Zhuo, S. Ye, S.T. Lee, Manganese dioxide modified silicon nanowires and their excellent catalysis in the decomposition of methylene blue, Appl. Phys. Lett. 100 (2012) 063104.
[27] Y. Qu, X. Zhong, Y. Li, L. Liao, Y. Huang, X. Duan, Photocatalytic properties of porous silicon nanowires, J. Mater. Chem. 20 (2010) 3590–3594.
[28] F.-Y. Wang, Q.-D. Yang, G. Xu, N.-Y. Lei, Y.K. Tsang, N.-B. Wong, J.C. Ho, Highly active and enhanced photocatalytic silicon nanowire arrays, Nanoscale 3 (2011) 3269–3276.
[29] N. Brahiti, T. Hadjersi, H. Menari, S. Amirouche, O. El Kechai, Enhanced photocatalytic degradation of methylene blue by metal-modified silicon nanowires, Mater. Res. Bull. 62 (2015) 30–36.
[30] O. Fellahi, M.R. Das, Y. Coffinier, S. Szunerits, T. Hadjersi, M. Maamache, R. Boukherroub, Silicon nanowire arrays-induced graphene oxide reduction under UV irradiation, Nanoscale 3 (2011) 4662–4669.
[31] G. Piret, Y. Coffinier, C. Roux, O. Melnyk, R. Boukherroub, Biomolecule and nanoparticle transfer on patterned and heterogeneously wetted superhydrophobic silicon nanowire surfaces, Langmuir 24 (2008) 1670–1672.
[32] G. Piret, H. Drobecq, Y. Coffinier, O. Melnyk, R. Boukherroub, Matrix-free laser desorption/ionization mass spectrometry on silicon nanowire arrays prepared by chemical etching of crystalline silicon, Langmuir 26 (2010) 1354–1361.
[33] E. Galopin, J. Barbillat, Y. Coffinier, S. Szunerits, R. Boukherroub, Silicon nanowires coated with silver nanostructures as ultrasensitive interface for surface-enhanced Raman spectroscopy, ACS Appl. Mater. Interfaces 1 (2009) 1396–1403.
[34] H. Morinaga, M. Suyama, T. Ohmi, Mechanism of metallic particle growth and metal-induced pitting on Si wafer surface in wet chemical processing, J. Electrochem. Soc. 141 (1994) 2834–2841.
[35] M.Y. Abdul Halim, W.L. Tan, N.H.H. Abu Bakar, M. Abu Bakar, Surface characteristics and catalytic activity of copper deposited porous silicon powder, Materials 7 (2014) 7737–7751.
[36] H. Bandarenka, S.L. Prischepa, R. Fittipaldi, A. Vecchione, P. Nenzi, M. Balucani, V. Bondarenko, Comparative study of initial stages of copper immersion deposition on bulk and porous silicon, Nanoscale Res. Lett. 8 (2013) 85.
[37] Y. Coffinier, G. Piret, M.R. Das, R. Boukherroub, Effect of surface roughness and chemical composition on the wetting properties of silicon-based substrates, C.R. Chim. 16 (2013) 65–72.
[38] G. Piret, E. Galopin, Y. Coffinier, R. Boukherroub, D. Legrand, C. Slomianny, Culture of mammalian cells on patterned superhydrophilic/superhydrophobic silicon nanowire arrays, Soft Matter 7 (2011) 8642–8649.
[39] M.R. Prairie, L.R. Evans, B.M. Stange, S.L. Marlinez, An investigation of TiO_2 photocatalysis for the treatment of water contaminated with metals and organic chemicals, Environ. Sci. Technol. 27 (1993) 1776–1782.
[40] R. Katwal, H. Kaur, G. Sharma, Mu. Naushad, D. Pathania, Electrochemical synthesized copper oxide nanoparticles for enhanced photocatalytic and antimicrobial activity, J. Ind. Eng. Chem. 31 (2015) 173–184.
[41] J. Yang, Z. Li, C. Zhao, Y. Wang, X. Liu, Facile synthesis of Ag–Cu_2O composites with enhanced photocatalytic activity, Mater. Res. Bull. 60 (2014) 530–536.
[42] C.-K. Wu, M. Yin, S. O'Brien, J.T. Koberstein, Quantitative analysis of copper oxide nanoparticle composition and structure by X-ray photoelectron spectroscopy, Chem. Mater. 18 (2006) 6054–6058.
[43] M.C. Biesinger, L.W.M. Lau, A.R. Gerson, R. St.C. Smart, Resolving surface chemical states in XPS analysis of first row transition metals, oxides and hydroxides: Sc, Ti, V, Cu and Zn, Appl. Surf. Sci. 257 (2010) 887–898.
[44] Q. Wang, Q. Wang, M. Li, S. Szunerits, R. Boukherroub, Preparation of reduced graphene oxide/Cu nanoparticle composites through electrophoretic deposition: application for nonenzymatic glucose sensing, RSC Adv. 5 (2015) 15861–15869.
[45] G. Colon, M.C. Hidalgo, J.A. Navıo, Influence of carboxylic acid on the photocatalytic reduction of Cr(VI) using commercial TiO_2, Langmuir 17 (2001) 7174–7177.

Please cite this article in press as: O. Fellahi, et al., Reduction of Cr(VI) to Cr(III) using silicon nanowire arrays under visible light irradiation, J. Hazard. Mater. (2015), http://dx.doi.org/10.1016/j.jhazmat.2015.11.020